

**RESEARCH ARTICLE**

# Convective rain cell properties and the resulting precipitation scaling in a warm-temperate climate

Christopher Purr<sup>1</sup>  | Erwan Brisson<sup>1,2</sup>  | K. Heinke Schlünzen<sup>3</sup>  | Bodo Ahrens<sup>1</sup> 

<sup>1</sup>Institute for Atmospheric and Environmental Sciences, Goethe University Frankfurt, Frankfurt, Germany

<sup>2</sup>Centre National de Recherches Météorologiques, Toulouse, France

<sup>3</sup>Meteorological Institute, CEN, Universität Hamburg, Hamburg, Germany

**Correspondence**

Christopher Purr, Institute for Atmospheric and Environmental Sciences, Goethe University Frankfurt, Altenhöferallee 1, 60438 Frankfurt, Germany.

Email: [purr@iau.uni-frankfurt.de](mailto:purr@iau.uni-frankfurt.de)

**Funding information**

We thank the “Hessisches Landesamt für Naturschutz, Umwelt und Geologie” and the “Rheinland-Pfalz Kompetenzzentrum für Klimawandelfolgen” for funding the project “Konvektive Gefährdung über Hessen und Rheinland-Pfalz” in the course of which the results of this paper were obtained.

**Abstract**

Convective precipitation events have been shown to intensify at rates exceeding the Clausius–Clapeyron rate (CC rate) of ca.  $7\% \text{ K}^{-1}$  under current climate conditions. In this study, we relate atmospheric variables (low-level dew point temperature, convective available potential energy, and vertical wind shear), which are regarded as ingredients for severe deep convection, to properties of convective rain cells (cell area, maximum precipitation intensity, lifetime, precipitation sum, and cell speed). The rain cell properties are obtained from a rain gauge-adjusted radar dataset in a mid-latitude region, which is characterized by a temperate climate with warm summers (Germany). Different Lagrangian cell properties scale with dew point temperature at varying rates. While the maximum precipitation intensity of cells scales consistently at the CC rate, the area and precipitation sum per cell scale at varying rates above the CC rate. We show that this super-CC scaling is caused by a covarying increase of convective available potential energy with dew point temperature. Wind shear increases the precipitation sum per cell mainly by increasing the spatial cell extent. From an Eulerian point of view, this increase is partly compensated by a higher cell velocity, which leads to Eulerian precipitation scaling rates close to and slightly above the CC rate. Thus, Eulerian scaling rates of convective precipitation are modulated by convective available potential energy and vertical wind shear, making it unlikely that present scaling rates can be applied to future climate conditions. Furthermore, we show that cells that cause heavy precipitation at fixed locations occur at low vertical wind shear and, thus, move relatively slowly compared to typical cells.

**KEYWORDS**

Clausius–Clapeyron scaling, convective storms, precipitation, tracking

## 1 | INTRODUCTION

Convective precipitation is expected to intensify with global warming (Trenberth et al., 2003). This intensification is also projected for warm-temperate climates in mid-latitudes (Purr et al., 2021). However, the rate of increase and the role of thermodynamic and dynamic processes remain uncertain. The water-holding capacity of the atmosphere, governed by the Clausius–Clapeyron (CC) equation, is frequently used as a baseline estimate for how much extreme precipitation will change with global warming (Westra et al., 2014). Two different approaches have been used to estimate the increase in extreme precipitation with temperature: *trend scaling* and *binning scaling*, sometimes also referred to as *apparent scaling* (Zhang et al., 2017). While *trend scaling* describes the ratio of precipitation extremes in different climate states scaled by the mean temperature change, *binning scaling* calculates the dependence of extreme precipitation on day-to-day temperature variability in the current climate period. *Binning scaling* has been frequently used in recent years due to a lack of long-term observations of sub-daily precipitation. *Binning scaling* rates above the CC rate of  $7\% \text{ K}^{-1}$  have been reported for convective precipitation extremes on sub-daily time scales in warm-temperate climate in a number of studies (e.g. Lenderink and van Meijgaard, 2008; Berg et al., 2013). Different explanations have been given for this super-CC scaling. Firstly, it has been attributed to a positive feedback mechanism between moisture supply at cloud base and updraft speed in convective clouds (Lenderink et al., 2017). Secondly, the increasing degree of convective organization at higher temperatures has been suggested to cause more intense precipitation (Moseley et al., 2016). This hypothesis has been established from idealized large eddy simulations (LES) which show that the precipitation field is organized into fewer but more intense precipitation cells at higher temperatures (Lochbihler et al., 2019). Additionally, the statistical effect that at high temperatures extreme precipitation is increasingly caused by convection was shown by Berg et al. (2013). The temperature scaling of both hourly extreme precipitation at fixed location (Prein et al., 2017) and of Lagrangian cell properties (Purr et al., 2019) has been shown to drop off at high temperature due to moisture limitation. Because of these varying scaling rates, dew point temperature has been suggested and widely adopted as a more meaningful covariate (Lenderink et al., 2011). It has been questioned whether binning scaling rates can be extrapolated to the future as other environmental conditions which influence convective storms beside low-level moisture might change, too (Bao et al., 2017; Sun et al., 2020). These environmental conditions, which determine the strength of a convective cell to a large

degree, are vertical instability, and vertical wind shear (see e.g. Weisman and Klemp, 1982 or Rasmussen and Blanchard, 1998). Vertical instability is often measured by convective available potential energy (CAPE). Although CAPE is useful for predicting the strength of convection it is mainly related to maximum vertical velocity in the updraft (Markowski and Richardson, 2010) and only indirectly to precipitation intensity. Precipitation intensity can be influenced by various additional processes, like entrainment rates and evaporation below cloud base. Precipitation efficiency, the ratio of total precipitation of a convective cloud to the moisture inflow at cloud base, has been shown to be strongly influenced by vertical wind shear (Weisman and Klemp, 1982; Market et al., 2003; Chen et al., 2015). In general, vertical wind shear influences the degree of organization of convective storms via various processes. Firstly, it increases the organization of convective storms by separating the updraft from the downdraft (and precipitation) region. Furthermore, it can facilitate the development of super cells by tilting horizontal vortices into the vertical and thus creating a rotating updraft. The spectrum of convective storms ranges from unorganized single convective cells at low wind shear via multi-cells, which are characterized by the repeated development of new cells in the vicinity of old ones, at intermediate wind shear to supercells and mesoscale convective systems at high wind shear (Houze Jr., 2014).

Beside increasing the severity of convective storms (Kaltenboeck and Steinheimer, 2015), high wind shear also increases the horizontal velocity of convective storms. Storm velocity increases because convective storms move approximately with the mean tropospheric wind and the commonly used bulk wind shear is largely determined by the wind at the 500 hPa level. In general, long-living cells are larger, more intense (Purr et al., 2019), and move faster. Because the high speed balances the higher precipitation intensity to some extent, it is not a priori clear to what extent intense fast-moving cells or less intense slow-moving cells cause heavy precipitation at fixed locations.

Due to their small spatial and temporal scale, convective storms are notoriously difficult to observe. When investigating extreme precipitation many observational studies rely on gauge data, although it has been shown that gauge datasets are only representative for spatial scales of up to 11 km for hourly accumulation periods (Bohnenstengel et al., 2011) and miss about 80% of hourly extreme precipitation events in Germany (Lengfeld et al., 2020) due to sparse sampling in space. Nonetheless, some interesting relations were found: for example, Lepore et al. (2016) investigated conditions leading to hourly precipitation extremes in the contiguous United States and found CAPE

and dew point temperature to be the best predictors for precipitation intensity.

The shortcomings of *in situ* measurements can be remedied by remote-sensing techniques to an ever increasing degree. Remote-sensing data used for investigating convective storms include lightning data (Wapler, 2013; Brisson et al., 2021) and weather radars (e.g. Moseley et al., 2013; Lochbihler et al., 2017). Kunz et al. (2020) combined radar data with storm reports and re-analysis data to investigate hailstorms in Central Europe. They found that vertical wind shear provides a good predictor for the size of hail stones as frontal storms associated with high wind shear tend to form larger hail stones. The progress of weather radars has made it possible to track convective storms in datasets that currently cover time periods of up to two decades (e.g. Peleg et al., 2018). While many studies track convective cells based on radar reflectivity, few radar datasets offer reliable estimates of ground-level precipitation. For this reason, Lagrangian properties of convective rain events have seldomly been quantitatively connected to precipitation at fixed locations. As an example of this kind of study, Schumacher and Johnson (2005) showed that about two-thirds of daily extreme precipitation is caused by Mesoscale Convective Systems (MCS) and investigated the MCS's properties.

The influence of the environmental conditions described above on storm properties has, to the authors' knowledge, not yet been studied in observational data on decadal time scales. Therefore, we attempt to establish a link between the influence of environmental conditions on storm properties focusing on the effect of wind shear on storm velocity and the resulting precipitation at fixed locations in this study. Beside process understanding, investigating the effect of large-scale environmental conditions on cell properties is beneficial in the context of model evaluation and climate change. Firstly, the results obtained here can be used for evaluating convective clouds in convection-permitting weather and climate models. While Purr et al. (2019) already evaluated the frequency distribution and temperature scaling of convective cells in a regional climate model (RCM), more thorough evaluation linking cell properties to environmental conditions would be advantageous. Additionally, convection parameterizations could be tested, especially with respect to the influence of wind shear on mesoscale organization (Yano and Moncrieff, 2016; Rio et al., 2019). In the context of climate change, linking convective cell properties to environmental conditions could be used to develop a statistical model, which allows deriving convective cell properties for future conditions from environmental variables provided by hydrostatic RCMs. Currently, these RCMs are used to investigate frequency changes in severe convection environments, which are usually defined as environments

with certain amounts of instability and wind shear without knowing how convective cells will react to the changes (Púčik et al., 2017). Therefore, we aim at answering the following questions:

1. What is the effect of instability and wind shear on Lagrangian cell properties and the dew point temperature scaling of these properties?
2. To what extent does higher cell velocity offset the higher organization of convective cells in high-shear environments with respect to precipitation at fixed location?

We use a novel, gauge-adjusted radar climatology, which provides continuous precipitation data in time and space. Properties of convective storms causing extreme sub-daily precipitation are investigated by tracking convective cells in 5-min radar data (Sections 2.1 and 3.1). To estimate the influence of wind shear, instability, and low-level moisture we connect the cell properties to the corresponding large-scale atmospheric conditions using ERA5 re-analysis data (Section 2.2). Re-analysis data are used instead of sounding data because of their high temporal and spatial frequency. While soundings are often taken only two or four times a day and hundreds of kilometers away from a convective storm, the ERA5 re-analysis provides hourly values at 0.25° resolution. For the United States, Lepore et al. (2015) found that rainfall intensity is better correlated with CAPE from re-analysis than with CAPE computed from atmospheric soundings. The results are presented in Section 4 for univariate and multivariate dependence of Lagrangian cell properties on environmental variables (Sections 4.1, 4.2), and thus question 1 is addressed. The relation of cell properties to precipitation at fixed locations, which addresses question 2, is provided in Section 4.3.

## 2 | DATA

### 2.1 | Radar climatology

We use the radar-based precipitation climatology (Winterrath et al., 2017) developed by the national meteorological service of Germany, Deutscher Wetterdienst, for tracking convective cells. This precipitation dataset is based on radar data, which have been quality-checked, corrected, and adjusted to rain gauge measurements. The correction steps used for this product to derive precipitation from radar reflectivity include clutter filtering, distance-dependent signal correction and removal of radar spokes. For the tracking we use the 5-min dataset, the so called YW product (Winterrath et al., 2018a). For

comparison to stationary hourly precipitation intensities, we use the hourly dataset, the so called RW product (Winterrath et al., 2018b). Our analysis covers the summer half years (April–September) of the period 2001–2016. Focusing on the summer half year is sufficient as convective rain events occur almost exclusively in this period (Lengfeld et al., 2021). The datasets have a spatial resolution of  $1 \text{ km} \times 1 \text{ km}$ .

## 2.2 | Environmental variables

We use ERA5, the fifth-generation global re-analysis by the European Centre for Medium-Range Weather Forecasts (ECMWF) (Hersbach et al., 2020), to derive environmental conditions of convective storms. The variables used to characterize convective storm conditions are dew point temperature at 2 m ( $T_d$ ), convective available potential energy (CAPE), and bulk vertical wind shear (SH) calculated as vector difference between the wind at the 500 hPa level and at 10 m. ERA5 provides hourly values of atmospheric variables at a spatial resolution of  $0.25^\circ \times 0.25^\circ$ . Convective parameters calculated from ERA5 data have been compared with sounding data and the MERRA-2 (Modern-Era Retrospective Analysis for Research and Applications version 2, Gelaro et al., 2017) re-analysis by Taszarek et al. (2020). ERA5 performs better than MERRA-2 for all variables but underestimates both mean and extreme values of CAPE and wind shear compared to atmospheric soundings.

An important consideration when relating cell properties to environmental conditions from re-analysis is the spatial and temporal representativeness of the re-analysis data. Precipitation scaling has been shown to depend on the timing of the temperature recording relative to the storm's occurrence (Lenderink et al., 2011). Downdrafts and evaporative cooling of rain associated with convective storms lead to a decrease in surface temperature. Visser et al. (2020) found that using sub-daily atmospheric conditions before the start of the storm for determining scaling rates results in increased consistency of the scaling rates. However, because we use a re-analysis that parameterizes convection it cannot be expected that the diurnal cycle of convective precipitation is perfectly represented. The convection parameterization might trigger precipitation prematurely which leads to depleted CAPE and decreased dew point temperature, and thus the environmental conditions before storm onset do not necessarily represent the determining conditions for storm development. For these reasons, we relate convective environmental conditions at two different times to cell properties. By default, we assign to each cell the three-hourly values of CAPE, SH, and  $T_d$

before storm onset at its onset location. Additionally, we test the influence of sub-daily variability by using daily mean values.

## 3 | METHODS

### 3.1 | Convective cell tracking

Because of its high temporal and spatial resolution, the radar data allow for a quasi-continuous monitoring of convective cells. We use a tracking algorithm to derive convective cell properties from the radar data. The algorithm is described in detail by Purrr et al. (2019). In summary, convective cells are tracked in three major steps:

1. Contiguous precipitation areas with precipitation intensity above a threshold of  $8.5 \text{ mm} \cdot \text{h}^{-1}$  (within 5 minutes), are identified in the current and the subsequent time step as potential convective objects. The minimum cell area is set to four grid points.
2. Wind information from the ERA5 re-analysis is used to predict the position of the cell at the subsequent time step. To this end, a “cone of detection” is set up for each pixel of every cell in the current time step. If a new cell is present in the cone, a probability value is assigned to the origin pixel of the cone, which links this pixel to the new cell.
3. The probability values of all pixels are summed up for each cell. If a single cell is present in the cone, the corresponding objects from the current and the subsequent time step are connected. If multiple cells are present, the current cell is associated with the cell with the highest probability in the subsequent time step.

Cells must have a lifetime of at least three time steps, i.e. of 15 min, to be considered for analysis. This precondition minimizes radar artifacts in the analysis. Cell mergers and splits are dealt with as follows: if two cells merge, the cell track with the higher probability of cell association is continued. The other track is regarded as an individual track. The same applies to cells that split. The properties that are obtained by the algorithm for each cell are: (1) lifetime; (2) mean intensity, i.e. the temporal and spatial mean over the entire lifetime; (3) maximum intensity, i.e. the highest grid point intensity during the entire lifetime; (4) maximum area, defined as the maximum instantaneous area over the entire lifetime; (5) precipitation sum, i.e. the total spatial and temporal precipitation sum over the entire lifetime; and (6) mean speed, defined as the temporal mean speed of the cells' center of mass. The center of mass is defined as the average position of all cell pixels, weighted according to their precipitation intensity. Figure 1 provides



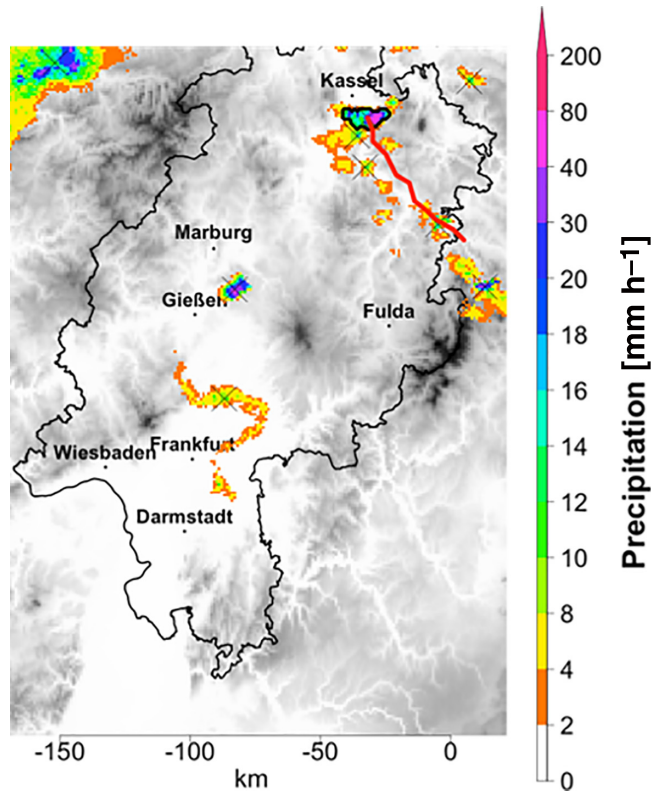


**FIGURE 1** Radar snapshot of a convective cell. Shown in color is the 5-min precipitation intensity on May 30, 2008 at 21:50 (UTC) and a detected cell track example as a red line. The track starts with cell detection at 21:00 (UTC) and is shown up to the time of the snapshot [Colour figure can be viewed at [wileyonlinelibrary.com](http://wileyonlinelibrary.com)]

an example of detected cells and a selected cell track (red line).

### 3.2 | Calculation of scaling rates

To investigate the influence of environmental conditions on cell properties, cells are grouped into 23 bins of dew point temperature, CAPE, or wind shear. The bin width varies in such a way that there is an approximately equal number of cells in each bin. As there are a total of ca. 1,350,000 cells in the area and period of investigation, there are about 60,000 cells in each bin.

The scaling rates  $s_p$  as function of dew point temperature  $T_d$  are computed for the highest percentiles  $p$  (90th, 95th, 99th, and 99.9th) of all cell properties as the average fractional change of the respective quantity (e.g. precipitation sum, maximum intensity, etc.)  $Q$  from bin  $i$  to bin  $i + 1$  as:

$$\bar{s}_p = \frac{\sum_{i=1}^{23} s_{p,i}}{23} = \ln \frac{Q_{p,i+1}}{Q_{p,i}} / (T_{d,i+1} - T_{d,i})$$

where  $T_{d,i}$  denotes dew point temperature of the respective bin  $i$ .

## 4 | RESULTS

### 4.1 | Univariate dependence of cell properties on environmental variables

The environmental variables influence the investigated cell properties maximum intensity, maximum area, and precipitation sum by varying degrees. In general, and as expected, an increase in CAPE or dew point temperature increases the severity of convective cells. Foremost, maximum intensity (Figure 2a, b) and area (Figure 2d, e) increase with these variables. To a lesser extent, lifetime of convective cells increases, too (Figure 2g, h). The 75th (99th) percentile of lifetime increases from 30 min (95 min) for CAPE values between 0 and  $0.75 \text{ J} \cdot \text{kg}^{-1}$  to 40 min (140 min) for CAPE values above  $1284 \text{ J} \cdot \text{kg}^{-1}$ . The maximum area of cells is relatively constant for low CAPE values up to  $\sim 200 \text{ J} \cdot \text{kg}^{-1}$  and increases for higher values. In contrast, it increases more uniformly with dew point temperature.

The maximum intensity increases approximately linearly with CAPE and exponentially with dew point temperature (note the varying bin widths in Figure 2a, b). Wind shear exerts a strong control on cell area (Figure 2f). While the 99th percentile of cell area is  $332 \text{ km}^2$  for the wind shear class  $0\text{--}2 \text{ m} \cdot \text{s}^{-1}$ , it is  $997 \text{ km}^2$  for wind shear above  $25 \text{ m} \cdot \text{s}^{-1}$ . Interestingly the maximum cell intensity decreases with wind shear (Figure 2c). As a result, the total precipitation sum per cell increases strongly with increasing CAPE and dew point temperature but only slightly with increasing wind shear (Figure 2j–l). The overall increase in maximum intensity and precipitation sum with CAPE is non-monotonic for very low CAPE values with decreasing values from  $0 \text{ J} \cdot \text{kg}^{-1}$  to  $10 \text{ J} \cdot \text{kg}^{-1}$ . This decrease is smaller when using daily mean CAPE values. For example, the 99th percentile of maximum intensity decreases from  $113 \text{ mm} \cdot \text{h}^{-1}$  for CAPE values between  $0 \text{ J} \cdot \text{kg}^{-1}$  and  $0.8 \text{ J} \cdot \text{kg}^{-1}$  to  $95 \text{ mm} \cdot \text{h}^{-1}$  for values between  $10 \text{ J} \cdot \text{kg}^{-1}$  and  $15.5 \text{ J} \cdot \text{kg}^{-1}$  when using CAPE values before storm onset whereas it increases from  $85 \text{ mm} \cdot \text{h}^{-1}$  to  $87 \text{ mm} \cdot \text{h}^{-1}$  when using daily mean CAPE values. The mean cell speed is constant across the dew-point range, decreases slightly with increasing CAPE values, and increases with wind shear (not shown). However, an increase in wind shear leads to a smaller increase in cell speed. While the median cell speed is  $7.0 \text{ m} \cdot \text{s}^{-1}$  in the  $0 \text{ m} \cdot \text{s}^{-1}$  wind shear bin it increases to  $14 \text{ m} \cdot \text{s}^{-1}$  for  $27.5 \text{ m} \cdot \text{s}^{-1}$  wind shear.

Maximum intensity scales consistently over the dew-point range at the CC rate, except for a slight increase in scaling rates towards higher  $T_d$  values, suggesting that maximum intensity is mainly constrained by moisture availability (Figure 3a). The scaling rates range from

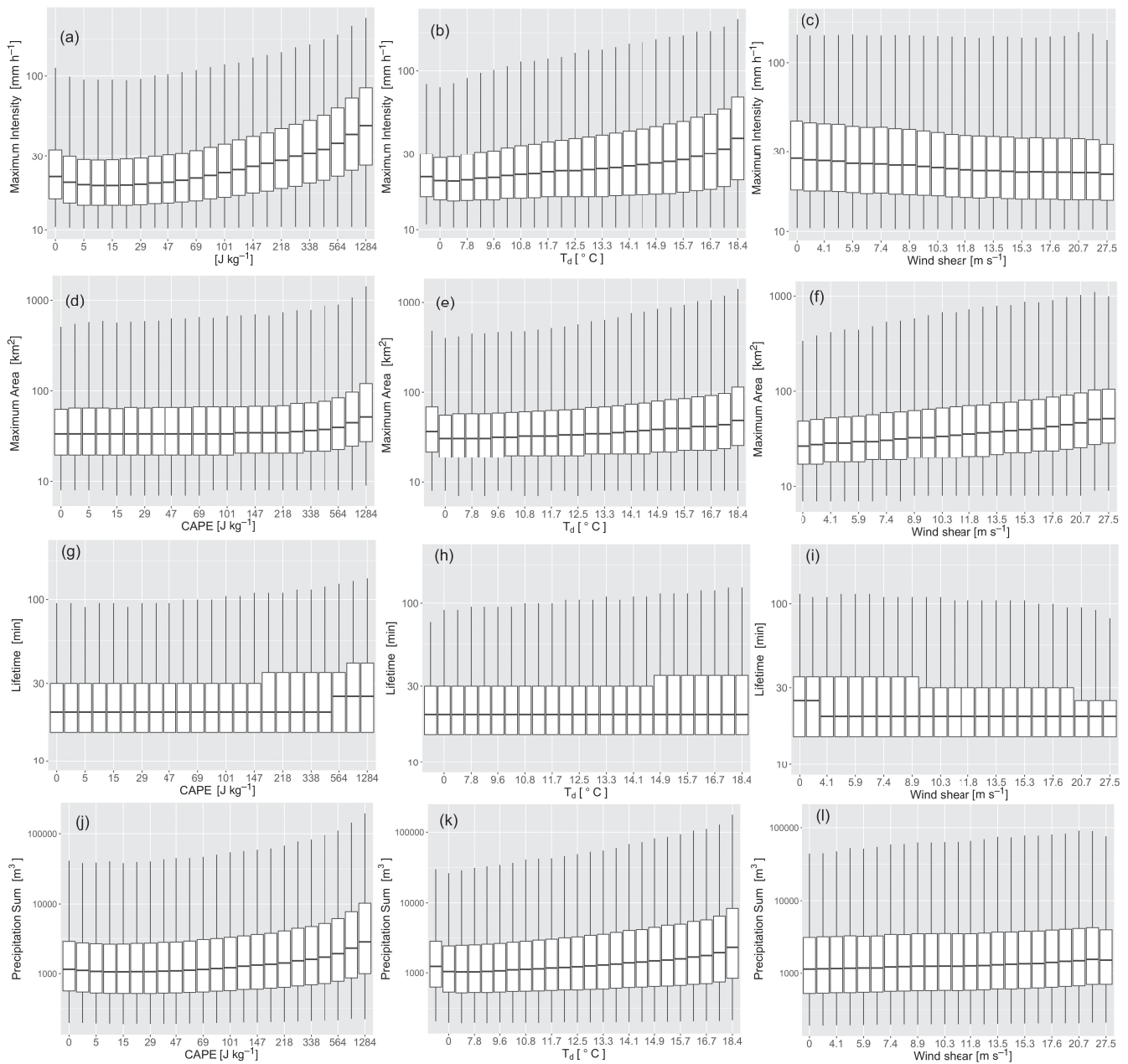


**FIGURE 2** Dependence of cell properties on environmental variables. Cells are grouped into bins as explained in Section 3.2. The lower and upper hinges denote the 25th and 75th percentiles respectively. The lower and upper whiskers denote the 1st and 99th percentiles respectively. Note the logarithmic y-axis and the varying bin widths on the x-axis, especially for the left column

$7.7\% \text{ K}^{-1}$  for  $s_{99}$  to  $8.0\% \text{ K}^{-1}$  for  $s_{95}$ . In contrast, cell area scales at different rates below and above a threshold of  $T_d \sim 12^\circ\text{C}$ . The scaling rates are below the CC rate below and at about two times the CC rate above this threshold (Figure 3b). Furthermore, the scaling rates of the different percentiles are more variable than for maximum intensity with values from  $8.4\% \text{ K}^{-1}$  for  $s_{90}$  to  $11.4\% \text{ K}^{-1}$  for  $s_{99.9}$ . These varying rates suggest that area is not controlled by dew point temperature alone and that the scaling rates are influenced by other variables like vertical wind shear.

Like cell area, the total precipitation sum also shows an increase in scaling rates with dew point temperature (Figure 3c). However, there is no distinct shift but a gradual increase of scaling rates from about the CC rate at low dew point temperatures to more than two times the CC rate at high dew point temperatures.

Using daily mean  $T_d$  instead of the value before storm onset does not change the shape of the scaling curves and influences the scaling rates only slightly. The scaling rates for maximum intensity increase to a range of  $8.1\% \text{ K}^{-1}$  ( $s_{99}$ )

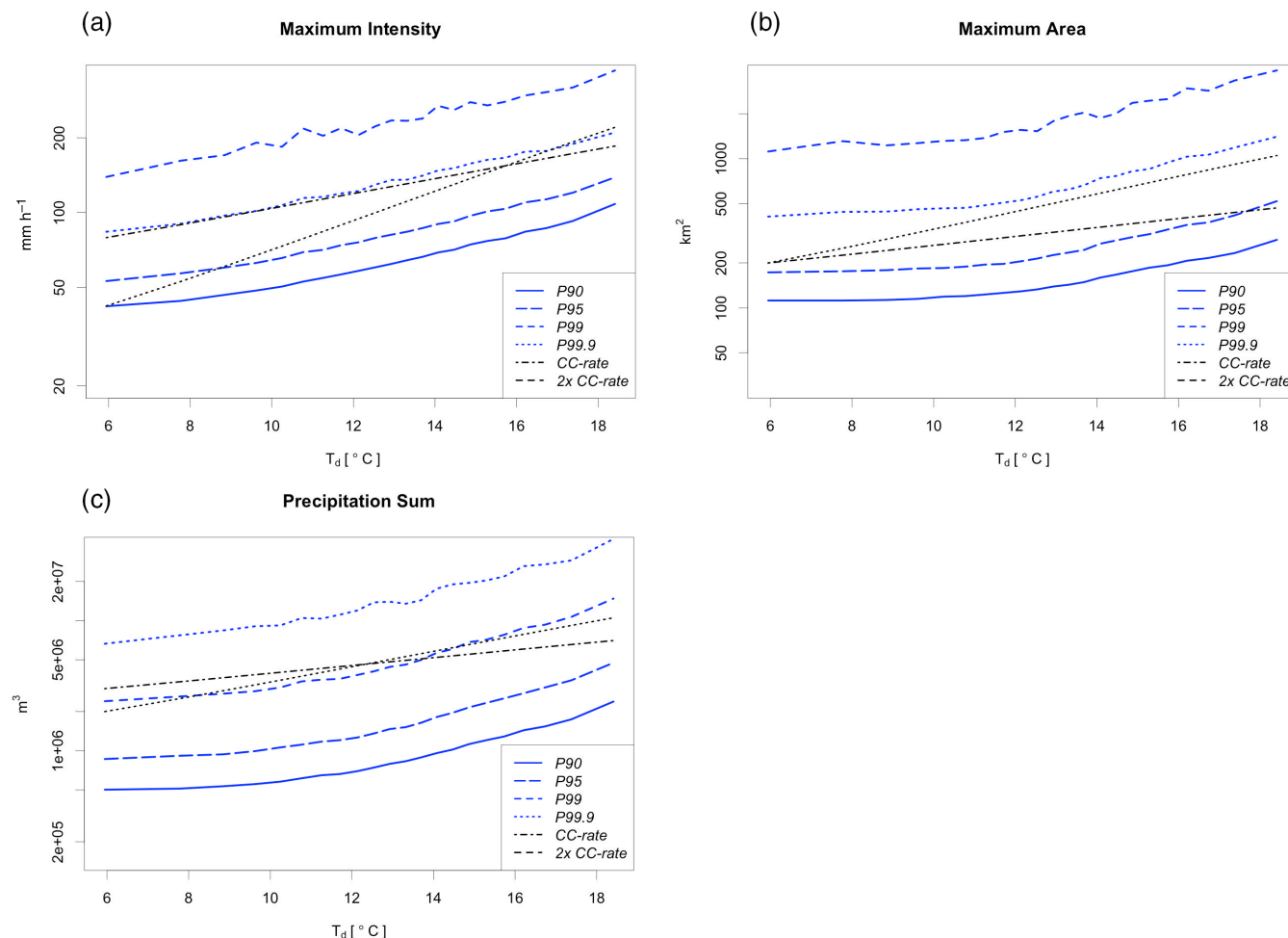


**FIGURE 3** Dew point temperature scaling of the cell properties (a) maximum intensity, (b) maximum area, and (c) precipitation sum (in blue). For orientation, the scaling CC rates and  $2 \times$  CC rates are given (black). Note the logarithmic y-axis [Colour figure can be viewed at [wileyonlinelibrary.com](http://wileyonlinelibrary.com)]

to  $8.5\% \text{ K}^{-1}$  ( $s_{99.9}$ ). The scaling rates for cell area and precipitation sum per cell using daily mean  $T_d$  are similar to the scaling rates using environmental conditions before storm onset.

Regarding a potential uncertainty estimation of scaling rates, the radar dataset does not provide error ranges. However, the dataset was evaluated against gauge data by Kreklow et al. (2020) who found an underestimation of high-intensity precipitation. As the highest precipitation intensities occur predominantly at high dew point temperatures, this underestimation implies that the radar-based scaling rates can be seen as the lower bound of the real scaling rates.

It has been shown that the occurrence of moderate hourly precipitation ( $>15 \text{ mm} \cdot \text{h}^{-1}$ ) is clearly coupled to orography, whereas extreme precipitation ( $>40 \text{ mm} \cdot \text{h}^{-1}$ ) is independent of orography (Lengfeld et al., 2019). For this reason, we separately investigated lowland and mountainous regions, defined as areas below or above

400 m elevation, to determine any differences in the scaling depending on orography. However, no difference in scaling between lowland and mountainous regions was found.

## 4.2 | Multivariate dependence of cell properties on environmental variables

We investigate cell properties and frequency of cells depending on combinations of environmental variables. In CAPE-SH space, the convective cells occur mainly at low CAPE, high wind shear values (SH) or high CAPE, low wind shear values (Figure 4a). While for low CAPE convection seems implausible at first sight, low-CAPE, high-shear convection is frequently observed in the US (see e.g. Sherburn et al., 2016). Besides, it cannot be completely ruled out that strong stratiform precipitation cells are detected by the tracking algorithm.

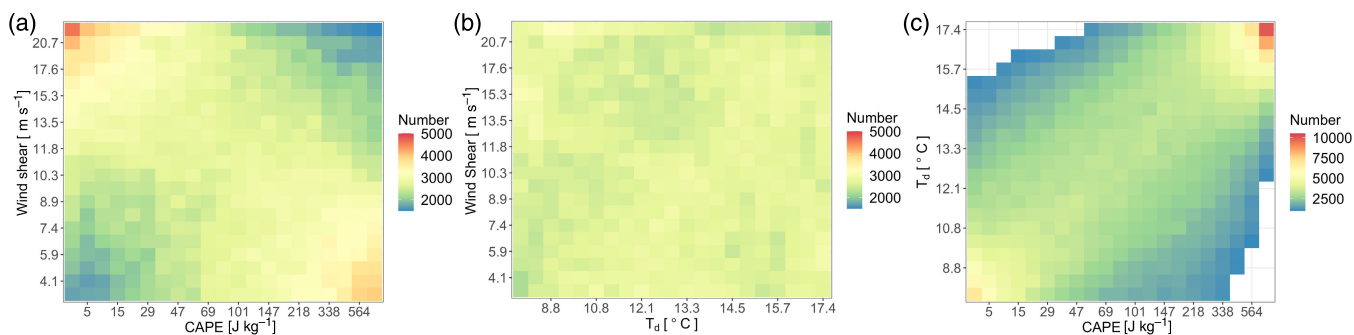


**FIGURE 4** (a–c) Occurrence of cells depending on values of the environmental variables convective available potential energy (CAPE), dew point temperature  $T_d$ , and wind shear SH. Note the colour bar in subfigure (c) is different [Colour figure can be viewed at [wileyonlinelibrary.com](http://wileyonlinelibrary.com)]

In  $T_d$ –SH space (Figure 4b), the cell numbers are approximately homogeneously distributed. However, there seems to be a slightly increased number of cells occurring at low  $T_d$  and high shear values, which are separated from cells occurring at higher  $T_d$  values. These cells could be related to fronts, which are characterized by high wind shear and may occur at low  $T_d$  values. In CAPE– $T_d$  space, the highest number of cells occurs at very high CAPE and  $T_d$  values. Furthermore, cells are concentrated along a corridor of increasing CAPE and  $T_d$  values (Figure 4c). The reason for this is that CAPE increases with  $T_d$ . We find an increase of the highest percentiles of daily maximum CAPE with daily  $T_d$  for all days of the investigation period 2001–2016 at varying rates well above the CC rate in the ERA5 re-analysis (Figure 5). The 95th percentile increases at rates around  $4 \times$  CC rate while the 99.9th percentile increases at around  $3 \times$  CC rate for dew point temperatures above  $7^\circ\text{C}$ . These values are well above the CC increase found in a simplified model which simulates peak CAPE under varying boundary layer moisture in a continental environment (Agard and Emanuel, 2017).

The most extreme cells, in terms of maximum intensity, maximum area, and precipitation sum, occur at high CAPE,  $T_d$ , and SH values (Figure 6). Low-CAPE, high-shear cells are not among the most extreme cells but have the lowest maximum intensity (Figure 6d). Again, wind shear is correlated predominantly with the area of cells (Figure 6a, c) and has little influence on the maximum intensity of cells (Figure 6d, f).

The influence of CAPE and wind shear on dew point temperature scaling is investigated by classifying convective cells according to their environmental CAPE and wind shear values. Cells are classified as “low CAPE” cells if they occur in conditions below the median value of  $87.5 \text{ J} \cdot \text{kg}^{-1}$ . Cells are classified as “high CAPE” cells if they occur at a higher value. Similarly, cells are classified as “low wind shear” cells if they occur at conditions below the median

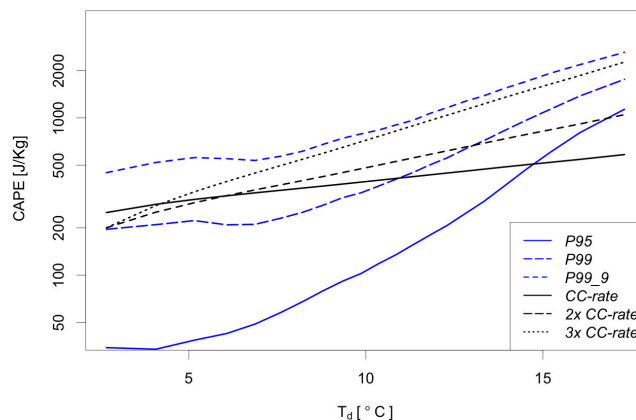


**FIGURE 5** Dew point temperature scaling of daily maximum convective available potential energy (CAPE). For orientation, the scaling CC,  $2 \times$  CC, and  $3 \times$  CC rates are given (black). Note the logarithmic y-axis [Colour figure can be viewed at [wileyonlinelibrary.com](http://wileyonlinelibrary.com)]

value of  $11.2 \text{ m} \cdot \text{s}^{-1}$ . If they occur at a higher value, they are classified as “high wind shear” cells. Classifying the cells according to environmental CAPE shows the effects of the general increase of CAPE with dew point temperature: cells which occur at low dew point temperatures occur predominantly at low CAPE values. Thus, the scaling curves of all cells shift gradually from the “low-CAPE” curve at low dew point temperatures to the “high CAPE” curve at high dew point temperatures (Figure 7a, c, e). The effect is smallest for the maximum area (Figure 7a), where it is only present for low dew point temperatures up to  $12^\circ\text{C}$ , and larger for the maximum intensity (Figure 7c) and the precipitation sum (Figure 7e).

Wind shear influences the scaling curves of the maximum area (Figure 7b) and the precipitation sum (Figure 7f) whereas there is little influence on the maximum intensity (Figure 7d). The scaling curves of the maximum area and the precipitation sum are at higher values for “high wind shear” cells which is in line with the



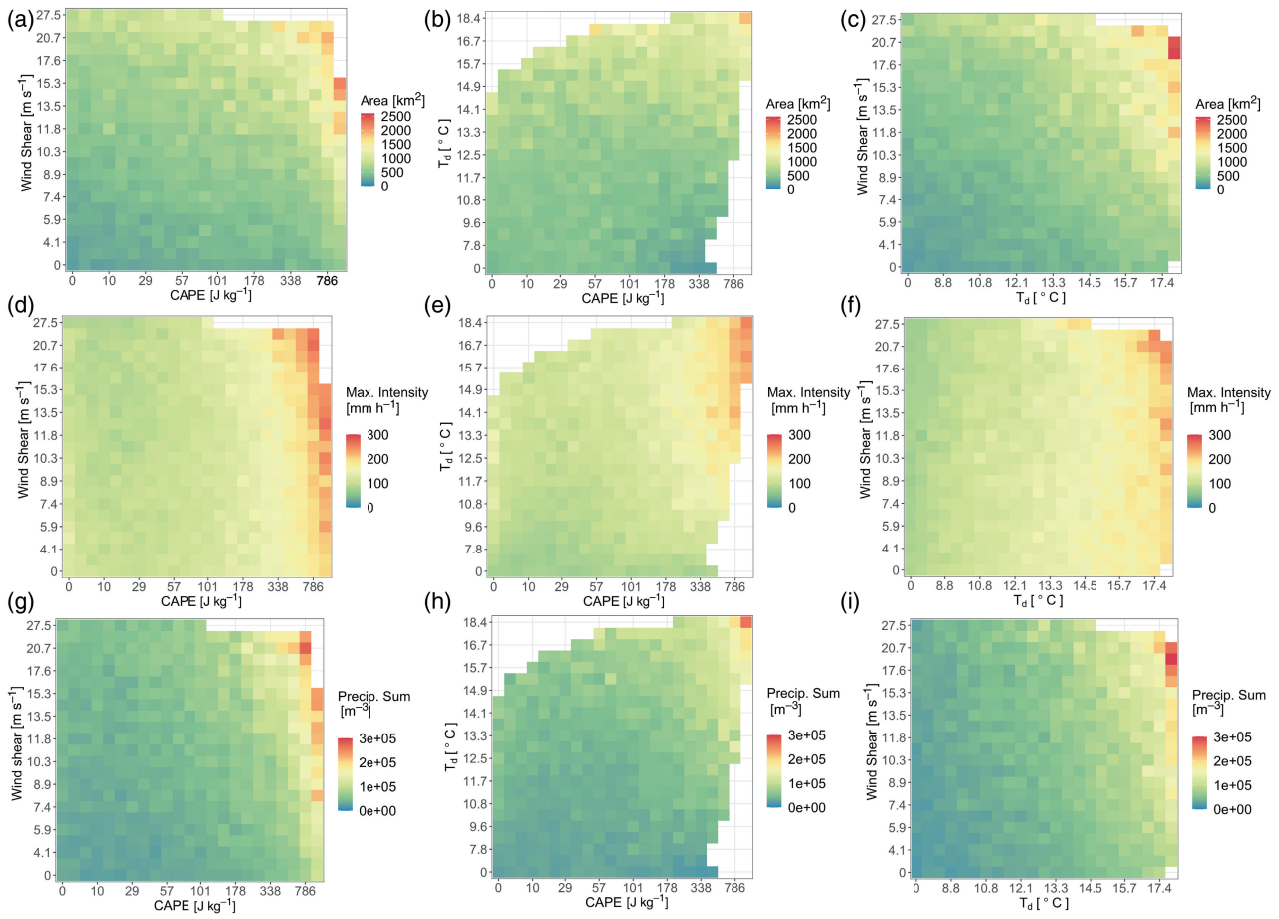


**FIGURE 6** 99th percentile of cell properties depending on the environmental variables convective available potential energy (CAPE), dew point temperature  $T_d$ , and wind shear SH [Colour figure can be viewed at [wileyonlinelibrary.com](https://onlinelibrary.wiley.com/doi/10.1002/qj.4277)]

findings in the previous section. In contrast to CAPE, the scaling rates do not differ between cells occurring at high or low wind shear conditions and all the cells.

### 4.3 | Relation of cell properties to precipitation at fixed location

We now investigate the relationship between Lagrangian cell properties and their potential to cause extreme precipitation for fixed locations. We use two methods to describe this relationship: (1) calculation of fixed location precipitation potential using Lagrangian cell properties; and (2) selection of all heavy precipitation events at fixed locations and investigation of the convective cells, which caused these extreme events.

#### 4.3.1 | Precipitation potential for fixed locations

To investigate the influence of wind shear on scaling for fixed location, we define the fixed location precipitation

potential  $P_{fl}$  for each cell. The purpose of this quantity is to derive a measure of how much each convective cell can precipitate at a fixed location based on its mean Lagrangian properties as derived from the tracking algorithm.  $P_{fl}$  is calculated as

$$P_{fl} = I * t = \min \left( I * \frac{D}{v}, I * l \right) = \min \left( I * \frac{2\sqrt{A}}{v\sqrt{\pi}}, I * l \right)$$

where  $I$  denotes the mean precipitation intensity,  $t$  the duration of precipitation,  $D$  the diameter calculated based on the mean area of the cell,  $v$  the mean speed,  $A$  the cell area and  $l$  the lifetime of the cell. The duration of the rain event at a fixed location is either calculated as the minimum of the diameter divided by the mean cell speed or taken as the cell lifetime. This condition accounts for the fact that a precipitation event at a fixed location can only last as long as the moving cell causing it.

$P_{fl}$  shows varying scaling regimes over the dew-point range (Figure 8a). It increases at rates below the CC rate for dew point temperatures below  $\sim 11^\circ\text{C}$  and slightly above

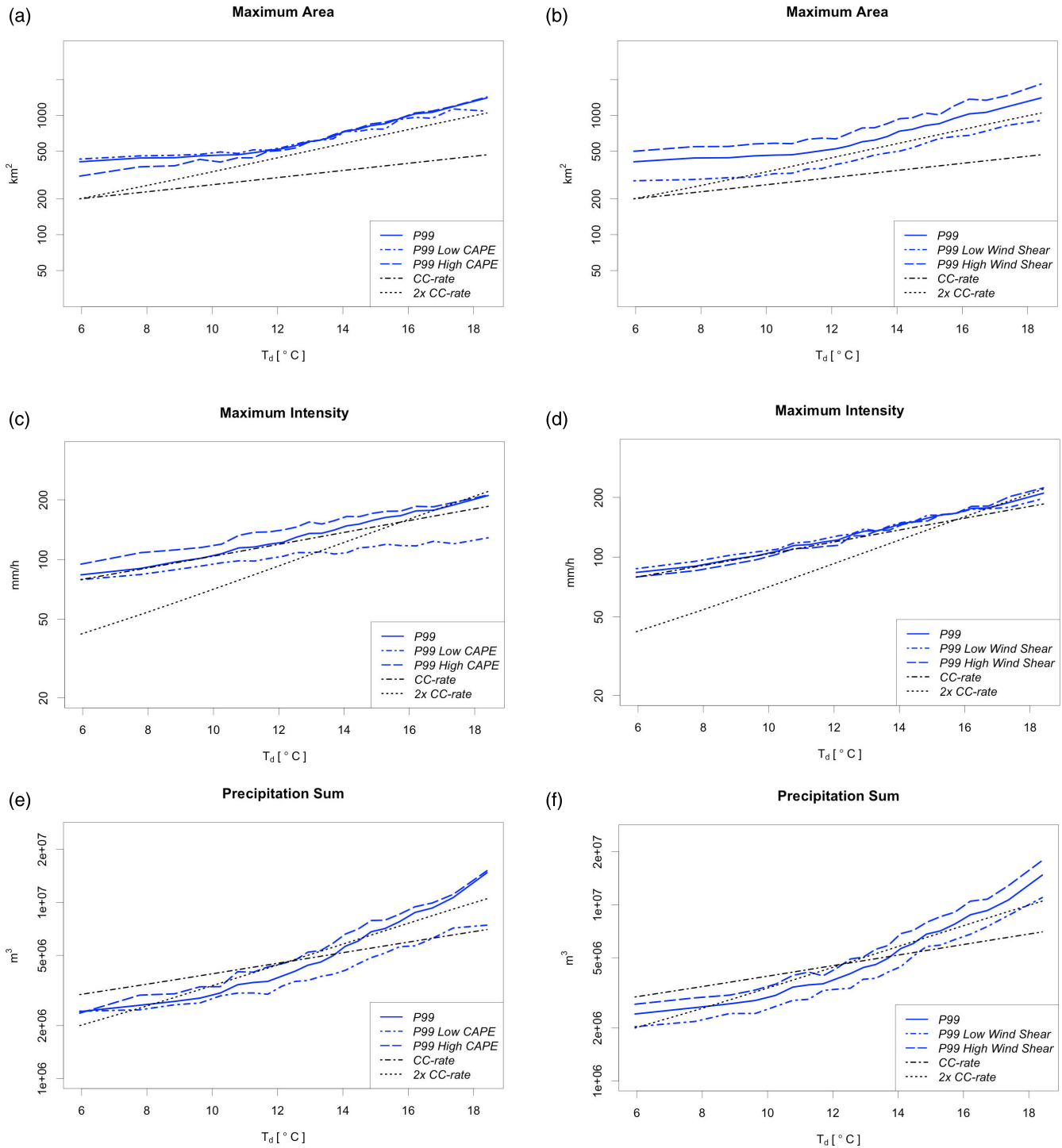


**FIGURE 7** Dew point scaling of the cell properties maximum area, maximum intensity, and precipitation sum (in blue) depending on convective available potential energy (CAPE) (left column), and wind shear (right column). For orientation, the scaling CC and  $2 \times$  CC rates are given (black). Note the logarithmic y-axis [Colour figure can be viewed at [wileyonlinelibrary.com](http://wileyonlinelibrary.com)]

the CC rate, at a rate of  $8.8\% \text{ K}^{-1}$ , above  $11^\circ\text{C}$ . The different percentiles increase at approximately similar rates. Concerning the influence of wind shear, the fixed location precipitation potential decreases with increasing wind shear (Figure 8b).

### 4.3.2 | Convective cells causing heavy precipitation events

We define heavy precipitation events at fixed locations as events with a precipitation amount of more than 25 mm

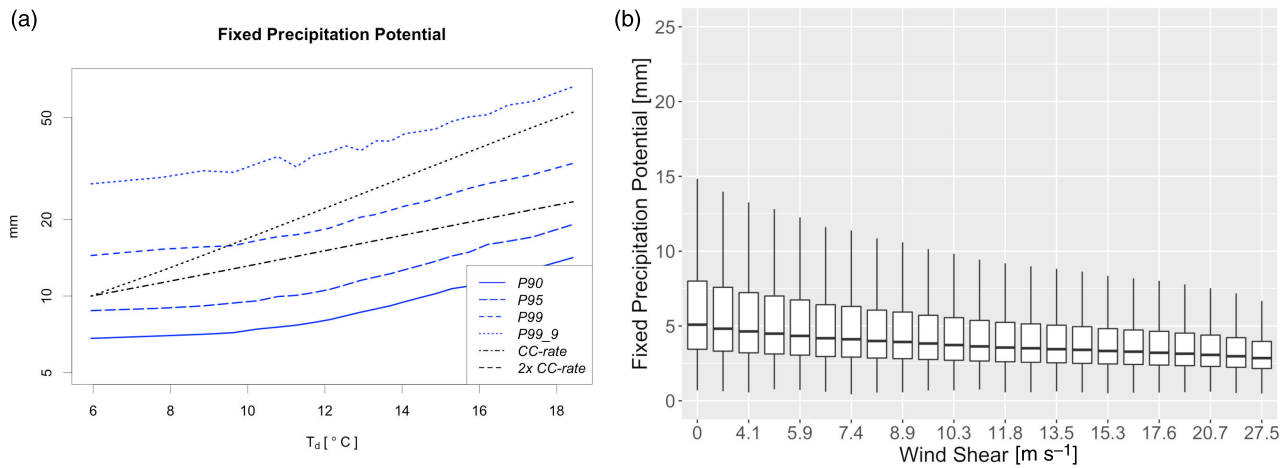


**FIGURE 8** (a) Scaling of fixed location precipitation potential with dew-point; (b) wind shear dependence of fixed location precipitation potential [Colour figure can be viewed at [wileyonlinelibrary.com](https://onlinelibrary.wiley.com)]

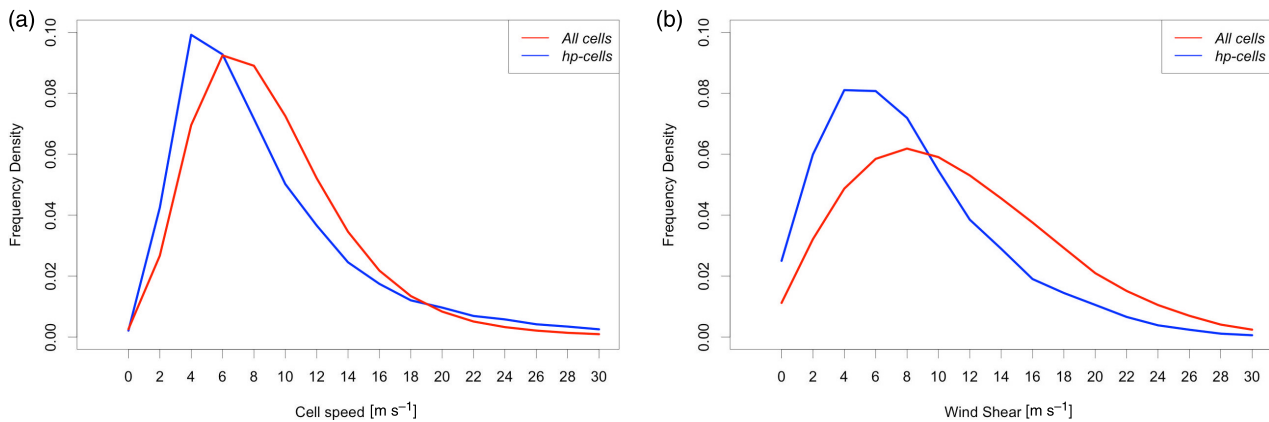


**FIGURE 9** Frequency densities of (a) cell speed of all cells and heavy precipitation (hp) cells, and (b) environmental wind shear for all cells and hp cells [Colour figure can be viewed at [wileyonlinelibrary.com](https://onlinelibrary.wiley.com)]

in 1 h within an area of  $1\text{ km}^2$  (equal to one grid box of the radar dataset). This definition follows the warning criterion for severe precipitation (at level 3 out of 4) of the Deutscher Wetterdienst. A convective cell is connected to a heavy precipitation event if it passes the grid box of heavy precipitation within the hour of its occurrence.

Cells that cause heavy precipitation at fixed locations (abbreviated as hp cells from now on) move comparably slow (Figure 9a). The median cell speed of hp cells is  $8.3\text{ m s}^{-1}$  compared to  $9.3\text{ m s}^{-1}$  for all cells. As cell speed is largely determined by wind shear, the frequency distribution of wind shear for hp cells is also shifted to lower values compared to all cells (Figure 9b).

## 5 | DISCUSSION AND CONCLUSION

We showed that Lagrangian cell properties scale with dew point temperature at varying rates under current climate

conditions. The maximum intensity of cells scales consistently at the CC rate, implying that the maximum intensity of cells is governed by thermodynamics. The area of cells increases at varying rates, namely at the CC rate below  $12^{\circ}\text{C}$  and at  $2\times\text{CC}$  rate above, which implicates a dynamic control. Indeed, cell area is strongly influenced by vertical wind shear, with higher wind shear leading to larger cells. This behavior reflects the well known increase of convective organization by vertical wind shear. In contrast, wind shear has very little influence on the maximum intensity of cells. The precipitation sum scales at above CC rate with higher scaling rates at higher dew point temperature. In summary, the strongest convective cells as measured by the precipitation sum per cell occur at high wind shear, high CAPE and high dew-point conditions.

Scaling for fixed location is lower than the Lagrangian scaling rate of total precipitation sum per cell due to the compensating effect of higher cell speed at high wind shear. The scaling rate of fixed precipitation potential ( $8.8\%\text{ K}^{-1}$ ) is in line with other studies which report

super-CC scaling for Germany (Berg et al., 2013; Ali et al., 2021). Thus, local differences in scaling rates of sub-daily precipitation at fixed location, which vary between the CC rate and  $2 \times$  CC rate, are modulated by differences in properties of convective storms. While we cannot distinguish between different processes discussed in the literature, like a positive feedback loop of cloud dynamics or the effect of self-organization in the current analyses, we point out that the increase of environmental CAPE with dew point temperature can serve as an explanation for super-CC scaling of sub-daily precipitation without assuming changes in the storm dynamics. Although it is well known that moist air is less dense, little attention has been paid to the fact that buoyancy (as measured by CAPE) increases with dew-point on climatological time scales when discussing super-CC scaling of sub-daily extreme precipitation. We conclude that super-CC scaling is at least partially caused by more unstable stratification of the pre-storm environment at high dew point temperatures.

The role of convective self-organization for the intensification of convective precipitation is currently an active area of research (e.g. Moseley et al., 2016; Lochbihler et al., 2019). Convective self-organization describes the process of convective cells to form clusters that tend to produce higher precipitation intensities and react differently to environmental conditions than unorganized convection. Often, convective self-organization is investigated by tracking precipitation and differentiating between cells that merge or split and solitary tracks. Preliminary analyses show that the average number of splits and mergers per cell increases consistently with increasing dew point temperature from ca. 0.2 splits and mergers per cell at 6°C to 0.95 at 19°C. Further investigations are needed to understand the role of mesoscale organization and the role of cold pools in detail.

The fact that scaling rates are modulated by vertical wind shear and CAPE makes it unlikely that present scaling rates for fixed locations can be transferred into the future. However, the results obtained in this paper can be used to infer how convective events might change by using a more quantitative description, like multivariate regression, of the relationship of cell properties to environmental conditions. As an alternative to purely statistical inference, convection-permitting climate simulations can be used to investigate changes in convective cells. As shown in Purrr et al. (2021), the dew-point scaling of convective cell properties is similar in present and future conditions for the highest percentiles. Thus, the dew-point scaling of cell properties shown in Section 4.1 might also be valid in the future climate. However, the frequency distribution of cells depending on dew point temperature changes. To understand the changes in the frequency distribution,

other variables might have to be taken into consideration. For example, changes in convective inhibition have been shown to change the population of convective cells in the future (Rasmussen et al., 2020). These changes potentially include a decreasing number of slow-moving convective cells in the afternoon (Purr et al., 2019). Combined with the fact that slow-moving cells have a higher potential for heavy precipitation at fixed location as shown in Section 4.3, this indicates a compensating effect on heavy precipitation. Again, this illustrates the fact that present scaling rates at fixed locations cannot simply be extrapolated into the future (Fowler et al., 2021). Future research should investigate the role of different formulations of convective parameters like storm relative helicity or lifted index to better understand the organization of convective storms. Furthermore, the role of fronts and convergence lines as trigger mechanisms and the effect of orography or urban areas for triggering and enhancing convective cells should be further investigated.


## ACKNOWLEDGEMENTS

We thank the German weather service (Deutscher Wetterdienst) for providing the radar data.

## AUTHOR CONTRIBUTIONS

**Christopher Purrr:** Conceptualization; data curation; formal analysis; investigation; methodology; visualization; writing – original draft. **Erwan Brisson:** Investigation; methodology; software; supervision; writing – review and editing. **K. Heinke Schlünzen:** Methodology; supervision; validation; writing – review and editing. **Bodo Ahrens:** Conceptualization; funding acquisition; project administration; resources; supervision; writing – review and editing.

## ORCID

*Christopher Purrr*  <https://orcid.org/0000-0002-9376-432X>

*Erwan Brisson*  <https://orcid.org/0000-0003-2558-2556>

*K. Heinke Schlünzen*  <https://orcid.org/0000-0002-5711-547X>

*Bodo Ahrens*  <https://orcid.org/0000-0002-6452-3180>

## REFERENCES

- Agard, V. and Emanuel, K. (2017) Clausius–Clapeyron scaling of peak CAPE in continental convective storm environments. *Journal of the Atmospheric Sciences*, 74(9), 3043–3054. <https://doi.org/10.1175/JAS-D-16-0352.1>.
- Ali, H., Fowler, H.J., Lenderink, G., Lewis, E. and Pritchard, D. (2021) Consistent large-scale response of hourly extreme precipitation to temperature variation over land. *Geophysical Research Letters*, 48, e2020GL090317. <https://doi.org/10.1029/2020GL090317>.



- Bao, J., Sherwood, S., Alexander, L. et al. (2017) Future increases in extreme precipitation exceed observed scaling rates. *Nature Climate Change*, 7, 128–132. <https://doi.org/10.1038/nclimate3201>
- Berg, P., Moseley, C. and Haerter, J. (2013) Strong increase in convective precipitation in response to higher temperatures. *Nature Geoscience*, 6, 181–185. <https://doi.org/10.1038/ngeo1731>.
- Brisson, E., Blahak, U., Lucas-Picher, P., Purrr, C. and Ahrens, B. (2021) Contrasting lightning projection using the lightning potential index adapted in a convection-permitting regional climate model. *Climate Dynamics*, 57, 2037–2051. <https://doi.org/10.1007/s00382-021-05791-z>.
- Bohnenstengel, S.I., Schlünzen, K.H. and Beyrich, F. (2011) Representativity of in-situ precipitation measurements – a case study for the LITFASS area in north-eastern Germany. *Journal of Hydrology*, 400(3–4), 387–395. <https://doi.org/10.1016/j.jhydrol.2011.01.052>.
- Chen, Q., Fan, J., Hagos, S., Gustafson, W.I., Jr. and Berg, L.K. (2015) Roles of wind shear at different vertical levels: cloud system organization and properties. *Journal of Geophysical Research – Atmospheres*, 120, 6551–6574. <https://doi.org/10.1002/2015JD023253>.
- Fowler, H.J., Lenderink, G., Prein, A.F., Westra, S., Allan, R.P., Ban, N., Barbero, R., Berg, P., Blenkinsop, S., Do, H.X., Guerreiro, S., Haerter, J.O., Kendon, E.J., Lewis, E., Schaer, C., Sharma, A., Villarini, G., Wasko, C. and Zhang, X. (2021) Anthropogenic intensification of short-duration rainfall extremes. *Nature Reviews Earth and Environment*, 2, 107–122. <https://doi.org/10.1038/s43017-020-00128-6>.
- Gelaro, R., McCarty, W., Suárez, M.J., Todling, R., Molod, A., Takacs, L., Randles, C.A., Darmenov, A., Bosilovich, M.G., Reichle, R., Wargan, K., Coy, L., Cullather, R., Draper, C., Akella, S., Buchard, V., Conaty, A., da Silva, A.M., Gu, W., Kim, G., Koster, R., Lucchesi, R., Merkova, D., Nielsen, J.E., Partyka, G., Pawson, S., Putman, W., Rienecker, M., Schubert, S.D., Sienkiewicz, M. and Zhao, B. (2017) The modern-era retrospective analysis for research and applications, version 2 (MERRA-2). *Journal of Climate*, 30(14), 5419–5454. <https://doi.org/10.1175/JCLI-D-16-0758.1>.
- Hersbach, H. and Coauthors. (2020) The ERA5 global reanalysis. *Quarterly Journal of the Royal Meteorological Society*, 810, 1–51. <https://doi.org/10.1002/qj.3803>.
- Houze, R.A., Jr. (2014) *Cloud Dynamics*, 2nd edition. San Diego, CA: Elsevier/Academic Press, ISBN, 9780123742667.
- Kreklow, J., Tetzlaff, B., Burkhard, B. and Kuhnt, G. (2020) Radar-based precipitation climatology in Germany—developments, uncertainties and potentials. *Atmosphere*, 11(2), 217. <https://doi.org/10.3390/atmos11020217>.
- Kunz, M., Wandel, J., Fluck, E., Baumstark, S., Mohr, S. and Schemm, S. (2020) Ambient conditions prevailing during hail events in Central Europe. *Natural Hazards and Earth System Sciences*, 20(6), 1867–1887. <https://doi.org/10.5194/nhess-20-1867-2020>.
- Kaltenboeck, R. and Steinheimer, M. (2015) Radar-based severe storm climatology for Austrian complex orography related to vertical wind shear and atmospheric instability. *Atmospheric Research*, 158–159, 216–230. <https://doi.org/10.1016/j.atmosres.2014.08.006>.
- Lenderink, G. and van Meijgaard, E. (2008) Increase in hourly precipitation extremes beyond expectations from temperature changes. *Nature Geoscience*, 1, 511–514. <https://doi.org/10.1038/ngeo262>.
- Lenderink, G., Mok, H., Lee, T. and Van Oldenborgh, G. (2011) Scaling and trends of hourly precipitation extremes in two different climate zones—Hong Kong and The Netherlands, *Hydrol. Earth System Science*, 15(9), 3033–3041. <https://doi.org/10.5194/hessd-8-4701-2011>.
- Lenderink, G., Barbero, R., Loriaux, J.M. and Fowler, H.J. (2017) Super-Clausius-Clapeyron scaling of extreme hourly convective precipitation and its relation to large-scale atmospheric conditions. *Journal of Climate*, 30(15), 6037–6052. <https://doi.org/10.1175/JCLI-D-16-0808.1>.
- Lengfeld, K., Winterrath, T., Junghänel, T. and Hafer, M. (2019) Characteristic spatial extent of hourly and daily precipitation events in Germany derived from 16 years of radar data, 28(5), 363–378. <https://doi.org/10.1127/metz/2019/0964>.
- Lengfeld, K., Kirstetter, P.E., Fowler, H.J., Yu, J., Becker, A., Flamig, Z. and Gourley, J. (2020) Use of radar data for characterizing extreme precipitation at fine scales and short durations. *Environmental Research Letters*, 15, 085003. <https://doi.org/10.1088/1748-9326/ab98b4>.
- Lengfeld, K., Walawender, K., Winterrath, T. and Becker, A. (2021) CatRaRE: a catalogue of radar-based heavy rainfall events in Germany derived from 20 years of data. *Meteorologische Zeitschrift*, 30(6), 469–487. <https://doi.org/10.1127/metz/2021/1088> 2021.
- Lepore, C., Veneziano, D. and Molini, A. (2015) Temperature and CAPE dependence of rainfall extremes in the eastern United States. *Geophysical Research Letters*, 42, 74–83. <https://doi.org/10.1002/2014GL062247>.
- Lepore, C., Allen, J.T. and Tippett, M.K. (2016) Relationships between hourly rainfall intensity and atmospheric variables over the contiguous United States. *Journal of Climate*, 29(9), 3181–3197. <https://doi.org/10.1175/JCLI-D-15-0331.1>.
- Lochbihler, K., Lenderink, G. and Siebesma, A.P. (2017) The spatial extent of rainfall events and its relation to precipitation scaling. *Geophysical Research Letters*, 44, 8629–8636. <https://doi.org/10.1002/2017GL074857>.
- Lochbihler, K., Lenderink, G. and Siebesma, A.P. (2019) Response of extreme precipitating cell structures to atmospheric warming. *Journal of Geophysical Research: Atmospheres*, 124, 6904–6918. <https://doi.org/10.1029/2018JD029954>.
- Market, P., Allen, S., Scofield, R., Kuligowski, R. and Gruber, A. (2003) Precipitation efficiency of warm-season Midwestern mesoscale convective systems. *Weather and Forecasting*, 18(6), 1273–1285. [https://doi.org/10.1175/1520-0434\(2003\)018<1273:PEOWMM>2.0.CO;2](https://doi.org/10.1175/1520-0434(2003)018<1273:PEOWMM>2.0.CO;2).
- Markowski & Richardson. (2010) *Mesoscale Meteorology in Midlatitudes*. Chichester, UK: Wiley-Blackwell, p. 43.
- Moseley, C., Berg, P. and Haerter, J.O. (2013) Probing the precipitation life cycle by iterative rain cell tracking. *Journal of Geophysical Research – Atmospheres*, 118, 13,361–13,370. <https://doi.org/10.1002/2013JD020868>.
- Moseley, C., Hohenecker, C., Berg, P. and Haerter, J.O. (2016) Intensification of convective extremes driven by cloud–cloud interaction. *Nature Geoscience*, 9, 748–752. <https://doi.org/10.1038/ngeo2789>.
- Peleg, N., Marra, F., Fatichi, S., Molnar, P., Morin, E., Sharma, A. and Burlando, P. (2018) Intensification of convective rain cells at warmer temperatures observed from high-resolution weather radar data. *Journal of Hydrometeorology*, 19, 715–726. <https://doi.org/10.1175/JHM-D-17-0158.1>.

- Prein, A., Rasmussen, R., Ikeda, K., et al. (2017) The future intensification of hourly precipitation extremes. *Nature Climate Change*, 7, 48–52. <https://doi.org/10.1038/nclimate3168>.
- Pučík, T., Groenemeijer, P., Rädler, A.T., Tijssen, L., Nikulin, G., Prein, A.F., van Meijgaard, E., Fealy, R., Jacob, D. and Teichmann, C. (2017) Future changes in European severe convection environments in a regional climate model ensemble. *Journal of Climate*, 30, 6771–6794. <https://doi.org/10.1175/JCLI-D-16-0777.1>.
- Purr, C., Brisson, E. and Ahrens, B. (2019) Convective shower characteristics simulated with the convection-permitting climate model COSMO-CLM. *Atmosphere*, 10(12), 810. <https://doi.org/10.3390/atmos10120810>.
- Purr, C., Brisson, E. and Ahrens, B. (2021) Convective rain cell characteristics and scaling in climate projections for Germany. *International Journal of Climatology*, 41, 3174–3185. <https://doi.org/10.1002/joc.7012>.
- Rasmussen, E. and Blanchard, D. (1998) A baseline climatology of sounding-derived supercell and tornado forecast parameters. *Weather and Forecasting*, 13, 1148–1164. [https://doi.org/10.1175/1520-0434\(1998\)013<1148:ABCOSD>2.0.CO;2](https://doi.org/10.1175/1520-0434(1998)013<1148:ABCOSD>2.0.CO;2).
- Rasmussen, K.L., Prein, A.F., Rasmussen, R.M., Ikeda, K. and Liu, C. (2020) Changes in the convective population and thermodynamic environments in convection-permitting regional climate simulations over the United States. *Climate Dynamics*, 55, 383–408. <https://doi.org/10.1007/s00382-017-4000-7>.
- Rio, C., Del Genio, A.D. and Hourdin, F. (2019) Ongoing breakthroughs in convective parameterization. *Current Climate Change Reports*, 5, 95–111. <https://doi.org/10.1007/s40641-019-00127-w>.
- Schumacher, R.S. and Johnson, R.H. (2005) Organization and environmental properties of extreme-rain-producing mesoscale convective systems. *Monthly Weather Review*, 133(4), 961–976. <https://doi.org/10.1175/MWR2899.1>.
- Sherburn, K.D., Parker, M.D., King, J.R. and Lackmann, G.M. (2016) Composite environments of severe and nonsevere high-shear, low-CAPE convective events. *Weather and Forecasting*, 31(6), 1899–1927, Accessed May 24, 2021. <https://doi.org/10.1175/WAF-D-16-0086.1>.
- Sun, Q., Zwiers, F., Zhang, X. and Li, G. (2020) A comparison of intra-annual and long-term trend scaling of extreme precipitation with temperature in a large-ensemble regional climate simulation. *Journal of Climate*, 33(21), 9233–9245. <https://doi.org/10.1175/JCLI-D-19-0920.1>.
- Taszarek, M., Pilgaj, N., Allen, J.T., Gensini, V., Brooks, H.E. and Szuster, P. (2020) Comparison of convective parameters derived from ERA5 and MERRA2 with rawinsonde data over Europe and North America. *Journal of Climate*, 1–55, 1–55. <https://doi.org/10.1175/JCLI-D-20-0484.1>.
- Trenberth, K.E., Dai, A.G. and Rasmussen, R.M. (2003) The changing character of precipitation. *Bulletin of the American Meteorological Society*, 84, 1205–1217. <https://doi.org/10.1175/BAMS-84-9-1205>.
- Visser, J.B., Wasko, C., Sharma, A. and Nathan, R. (2020) Resolving inconsistencies in extreme precipitation-temperature sensitivities. *Geophysical research letters*, 47, e2020GL089723. <https://doi.org/10.1029/2020GL089723>.
- Wapler, K. (2013) High-resolution climatology of lightning characteristics within Central Europe. *Meteorology and Atmospheric Physics*, 122, 175–184. <https://doi.org/10.1007/s00703-013-0285-1>.
- Weisman, M.L. and Klemp, J.B. (1982) The dependence of numerically simulated convective storms on vertical wind shear and buoyancy. *Monthly Weather Review*, 110, 504–520. [https://doi.org/10.1175/1520-0493\(1982\)110<0504:TDonSC>2.0.CO;2](https://doi.org/10.1175/1520-0493(1982)110<0504:TDonSC>2.0.CO;2).
- Westra, S., Fowler, H.J., Evans, J.P., Alexander, L.V., Berg, P., Johnson, F., Kendon, E.J., Lenderink, G. and Roberts, N.M. (2014) Future changes to the intensity and frequency of shortduration extreme rainfall. *Reviews of Geophysics*, 52, 522–555. <https://doi.org/10.1002/2014RG000464>.
- Winterrath, T., Brendel, C., Hafer, M., Junghänel, T., et al. (2017) Erstellung einer radargestützten Niederschlagsklimatologie. *Berichte des Deutschen Wetterdienstes*, 251.
- Winterrath Tanja; Brendel Christoph, Hafer Mario; Junghänel Thomas; Klameth Anna; Lengfeld Katharina; Walawender Ewelina; Weigl Elmar; Becker Andreas (2018a): RADKLIM version 2017.002: reprocessed quasi gauge-adjusted radar data, 5-minute precipitation sums (YW) [https://doi.org/10.5676/DWD/RADKLIM\\_YW\\_V2017.002](https://doi.org/10.5676/DWD/RADKLIM_YW_V2017.002)
- Winterrath Tanja; Brendel Christoph, Hafer Mario; Junghänel Thomas; Klameth Anna; Lengfeld Katharina; Walawender Ewelina; Weigl Elmar; Becker Andreas (2018b): RADKLIM version 2017.002: reprocessed gauge-adjusted radar data, one-hour precipitation sums (RW) [https://doi.org/10.5676/DWD/RADKLIM\\_RW\\_V2017.002](https://doi.org/10.5676/DWD/RADKLIM_RW_V2017.002)
- Yano, J. and Moncrieff, M.W. (2016) Numerical archetypal parameterization for mesoscale convective systems. *Journal of the Atmospheric Sciences*, 73(7), 2585–2602. <https://doi.org/10.1175/JAS-D-15-0207.1>.
- Zhang, X., Zwiers, F., Li, G., Wan, H. and Cannon, A.J. (2017) Complexity in estimating past and future extreme short-duration rainfall. *Nature Geoscience*, 10, 255–259. <https://doi.org/10.1038/ngeo2911>.

**How to cite this article:** Purr, C., Brisson, E., Schlünzen, K.H. & Ahrens, B. (2022) Convective rain cell properties and the resulting precipitation scaling in a warm-temperate climate. *Quarterly Journal of the Royal Meteorological Society*, 148(745), 1768–1781. Available from: <https://doi.org/10.1002/qj.4277>